

PAPER • OPEN ACCESS

## Enhanced resource assessment and atmospheric monitoring of the research wind farm WiValdi

To cite this article: Norman Wildmann *et al* 2022 *J. Phys.: Conf. Ser.* **2265** 022029

View the [article online](#) for updates and enhancements.

You may also like

- [Optimal Prediction of Atmospheric Turbulence by Means of the Weather Research and Forecasting Model](#)

Alohotsy Rafalimanana, Christophe Giordano, Aziz Ziad *et al.*

- [The SparSpec algorithm and the application to the detection of spatial periodicities in tokamaks: using memory with relaxation](#)

D Testa, H Carfantan and L M Perrone

- [High-resolution UV/Optical/IR Imaging of Jupiter in 2016–2019](#)

Michael H. Wong, Amy A. Simon, Joshua W. Tollefson *et al.*



## ECS Membership = Connection

**ECS membership connects you to the electrochemical community:**

- Facilitate your research and discovery through ECS meetings which convene scientists from around the world;
- Access professional support through your lifetime career;
- Open up mentorship opportunities across the stages of your career;
- Build relationships that nurture partnership, teamwork—and success!

**Join ECS!**

**Visit [electrochem.org/join](https://electrochem.org/join)**



# Enhanced resource assessment and atmospheric monitoring of the research wind farm WiValdi

**Norman Wildmann, Martin Hagen and Thomas Gerz**

Deutsches Zentrum für Luft- und Raumfahrt e.V., Institut für Physik der Atmosphäre,  
Oberpfaffenhofen, Germany

E-mail: [norman.wildmann@dlr.de](mailto:norman.wildmann@dlr.de)

**Abstract.** Prior to the installation of wind turbines at the Krummendeich research wind farm (referred to as WiValdi) which is developed by the German Aerospace Center (DLR), we conducted measurements with a Doppler wind lidar (DWL) and a microwave radiometer (MWR) for 16 months, starting in November 2020. The remote sensing data was validated against radiosonde measurements in a short-term campaign in September 2021. We present a statistical analysis of wind speed, direction, shear and veer as derived from the DWL as well as static stability from temperature retrievals of the MWR in comparison to model results of the New European Wind Atlas (NEWA). The observational data from 2021 shows a higher occurrence rate of winds from northwest in comparison to the longer-term statistics of NEWA (2011-2018). From the overall statistics, cases with the occurrence of low-level jets (LLJ) are detected and separated. The LLJs appear in 49% of the observed nights and predominantly in conditions with seaward wind direction. The LLJ increases shear and veer in the rotor swept area and thus the potential loads significantly. Future research at WiValdi will allow to analyse the effects of such load cases on the wind turbines in detail.

## 1. Introduction

The wind resource at a wind energy site can be determined by numerical model analysis, but is often supported by local measurements to increase confidence and accuracy. In addition to wind speed at hub height, turbulence parameters and wind shear are crucial parameters for wind turbine (WT) loads and power estimation. Recent studies showed that wind veer is also an important parameter, which is strongly dependent on atmospheric stability and has an impact on power production and wake deflection. A site assessment according to IEC 61400-15 [1] requires the consideration of these parameters throughout the prospective rotor area. However, in order to understand the physical processes of site-specific atmospheric conditions, typical measurements with cup anemometers, sonic anemometers or profiling lidars are not conclusive. In North Germany, the German Aerospace Center (DLR) currently constructs the Krummendeich Research Wind Farm WiValdi. To characterize the wind resource and the atmospheric conditions at the site, a long-range Doppler wind lidar (DWL) and a microwave radiometer (MWR) have been installed prior to any WT or measurement mast installation. Their task is to measure wind speed, turbulence, temperature and humidity throughout the full atmospheric boundary layer (ABL) over several months, covering all seasons. The location of WiValdi is subject to both, winds from the sea from northwest as well as seaward winds from southwest through east (Fig. 1). Recent studies in the German Bight of the North Sea revealed



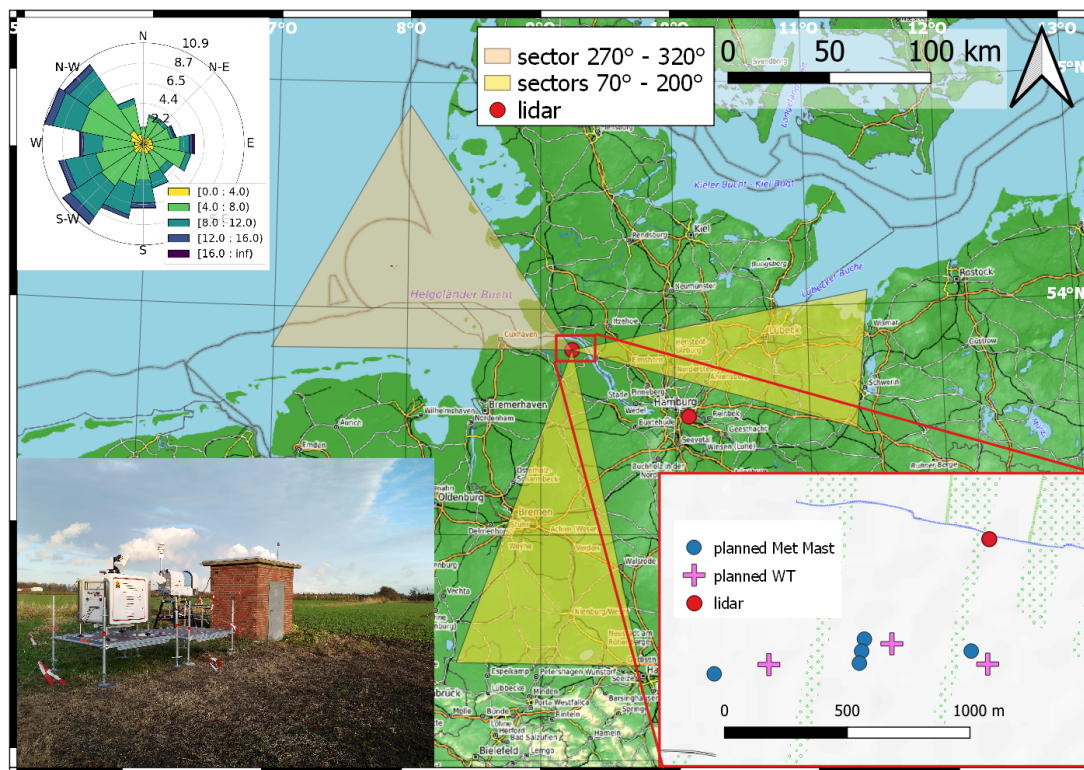


**Figure 1.** Map of North Germany with the locations of installed Doppler wind lidars, specific wind direction sectors, the measured overall wind rose and a picture of the Krümmendeich site. The map in the bottom right shows the lidar measurement position alongside the location of planned meteorological masts and wind turbines. Background map ©OpenTopoMap contributors 2022. Distributed under a Creative Commons BY-SA License.

that very specific stability conditions prevail depending on the wind direction. Platis et al. (2021) [3] used measurement data from FINO1 and FINO3 to show that stability conditions for landward winds from northwest are rarely stable, but seaward winds show a much larger percentage of stable conditions, which are unfavorable for wake recovery and can cause long wind farm wakes of tens of kilometers offshore. Emeis et al. (2016) [4] explained this weather feature with the passing of low pressure systems in the Northern Hemisphere, causing cold-sector winds from the northwest over the relatively warmer sea surface and warm sector winds from the southwest over the relatively cooler land surface at night. Kalverla et al. (2019) [5] analysed low-level jets (LLJs) in the North Sea and found a similar correlation to the wind direction. However, they assume that sea-breeze effects also play an important role for the development of LLJs particularly in coastal regions. In this study, we evaluate the wind conditions at the WiValdi site and evaluate if the observations there are comparable to the conditions in the German Bight and coastal regions. A specific focus of this study is on the evaluation of nighttime stable boundary layers, including the occurrences of low-level-jets (LLJs), which particularly impact the shear and veer loads of the rotor and can be of higher relevance for wake studies in the wind farm in future.

## 2. Objectives

The WiValdi research wind farm is designed to operate for at least 20 years and features a unique set of wind turbines which are equipped with an unprecedented amount of sensors. It is the goal

in this first meteorological study to build a database of remote sensing measurements which covers a wide range of meteorological conditions and can yield significant statistics of wind, turbulence and thermodynamic stratification. Beyond common wind resource assessment, the database shall contain information beyond the rotor area, covering the full ABL depths at best. In intensive operation periods (IOPs), the DWL and MWR measurements are complemented by eddy-covariance stations to obtain observations close to the ground, including fluxes of latent and sensible heat. Radiosondes and unmanned aerial systems (UAS) are operated on selected days for validation purposes. In light of this data, common weather patterns and the associated physical processes that lead to the wind and turbulence conditions in the wind farm can be better understood. A detailed knowledge and understanding of the atmospheric conditions associated to the site will enrich future research at WiValdi in multiple ways. A better understanding of wind direction- and stability-dependent loads can help to plan experiments and interpret the results. The measurements before installation of the turbines can later be used to analyse possible changes in local, micro-meteorological features of the site related to a change of sensible and latent heat surface fluxes or turbine-induced mixing.

### 3. Methodology

#### 3.1. Experiment description

The research wind park WiValdi is located in Northern Germany at the mouth of river Elbe and only approximately 40 km to the North Sea. Figure 1 shows the location on a map of North Germany. In the small map at the bottom right of Fig. 1, the location of the planned WT and meteorological mast installations is shown. The red dot indicates the temporary installation of a Doppler wind lidar (DWL) and a microwave radiometer (MWR) at the site. The instruments were installed in November 2020 and have since then collected a full year of data with only small periods of interruption due to power outages or instrument failure (see Sect. 4.1).

*3.1.1. Doppler wind lidar* To obtain vertical profiles of wind speed, direction and turbulence kinetic energy (TKE), the lidar is operating in velocity azimuth display (VAD) mode with two different elevation angles  $\varphi$ . A 30-minute period of VAD scans with  $\varphi = 75^\circ$  (VAD75) is followed by a 30-minute period of VAD scans with  $\varphi = 35.3^\circ$  (VAD35). The lower elevation angle allows to retrieve TKE according to Wildmann et al. 2020 [6], whereas the higher elevation angle scans feature a smaller footprint and reach up to higher altitudes which allow to cover the full boundary-layer depth in significantly more cases. The DWL operates with a physical resolution of approximately 50 m. The dead zone for the lidar is twice the physical resolution, so that the first range gate for radial velocity estimates is 100 m away from the lidar in line of sight direction. For the VAD35 that means that the lowest measurement height is 57 m, whereas for VAD75 it is at 96 m. To estimate shear and veer in the rotor plane, the VAD35 data are thus used, because they allow to calculate the parameters between 60 m and 140 m. Consequently, the VAD 35 data are also used to calculate the average wind speed and direction at hub height (i.e.  $\approx 100$  m).

*3.1.2. Microwave radiometer* Measurements by the MWR add information about temperature and humidity to the observational dataset. The MWR operates in a hybrid scanning scheme of zenith scans and boundary-layer scans, which allows a high resolution of measurements at low altitudes and a maximum height of 10.000 m.

A MWR is a purely passive remote sensing instrument. Vertical profiling with a MWR is achieved by measuring the atmospheric microwave emission along the wings of pressure broadened rotational lines. The 60 GHz oxygen absorption complex is used for temperature while the 22.4 GHz water vapor line is used for the humidity. The received brightness temperatures are fed into an artificial neural network or similar retrieval algorithm to solve

the nonlinear, underestimated problem of radiative transfer in a cloudy atmosphere and thus retrieve temperature and humidity profiles. The retrieval of temperature and humidity profiles from brightness temperatures is calibrated for the operational site with a large database of historic radiosonde soundings and model results [7]. The limitation of the retrieval algorithm, as to all statistical algorithms, is that they can only be applied to the range of atmospheric conditions, which is included in the training dataset, which is why long time series of historic data are needed, and a limited number of radiosonde data (e.g. from a short campaign) is not sufficient. The specified resolution and accuracy is as follows (from [8]):

- Tropospheric temperature profiles (0 – 10000 m): 200 m (< 5000 m altitude), 400 m above
  - profile accuracy:  $\pm 0.6$  K RMS (0-2000 m),  $\pm 1.0$  K RMS (> 2000 m)
- Boundary layer temperature profiles (0 – 1200 m), 30 m vertical resolution on the ground 50 m between 300 – 1200 m
  - profile accuracy:  $\pm 0.7$  K RMS
- Tropospheric humidity profiles (0 – 5000 m), 200 m vertical resolution (0 – 2000 m), 400 m (2000 – 5000 m)
  - profile accuracy:  $\pm 0.4$  g m<sup>-3</sup> RMS

The stratification of the atmosphere in the rotor area is determined as the potential temperature gradient  $\Delta\theta$  between 100 m and 150 m.

*3.1.3. Low-level jet detection* The occurrence of LLJs can be derived from lidar VAD scans with both elevation angles. Detection of LLJ-events is done through detection of wind speed maxima in the lowest 1000 m with a wind speed overshoot of 2 m s<sup>-1</sup> compared to the wind measurement at 1000 m, similar to the method of Kalverla et al. (2019) [5].

*3.1.4. Generated power estimation* For a rough estimate of potentially generated power at the site, the wind speed at hub height is used and applied to a simplified power curve. We assume a rated power of 4.3 MW at a rated wind speed of 13.1 m s<sup>-1</sup>. Cut-in wind speed is at 2.5 m s<sup>-1</sup>, cut-off wind speed is at 25 m s<sup>-1</sup>. In the partial load range, a linear relationship between wind speed and power is assumed. The wind turbines that will be installed at the site will have similar characteristics.

## 4. Results

### 4.1. Availability

From December 2020 to December 2021, the availability of lidar measurements with  $\varphi = 35^\circ$  ( $\varphi = 75^\circ$ ) at 100 m above ground level (AGL) was at 81% (90%) with approximately 3% data loss due to power or instrument failures and 16% due to bad weather conditions (mostly fog and rain). The availability decreases with height, due to lower CNR, low clouds and precipitation. During the night, an availability of 77% (86%) is still reached at 200 m AGL and 63% (76%) at 500 m. During the day, the availability at 500 m AGL is 72% (84%) and decreases to only 42% (66%) at 1000 m AGL. Since a reliable estimate of boundary layer height cannot be retrieved from lidar and MWR at all times, we assume that the 200 m level at night and 1000 m level at daytime are representative for measurements through the largest part of the ABL. The MWR availability is slightly lower than for the lidar at the 100 m level (80 %) due to a considerable higher amount of power failures, but it provides data for the whole height range from 0-10 km at all times.

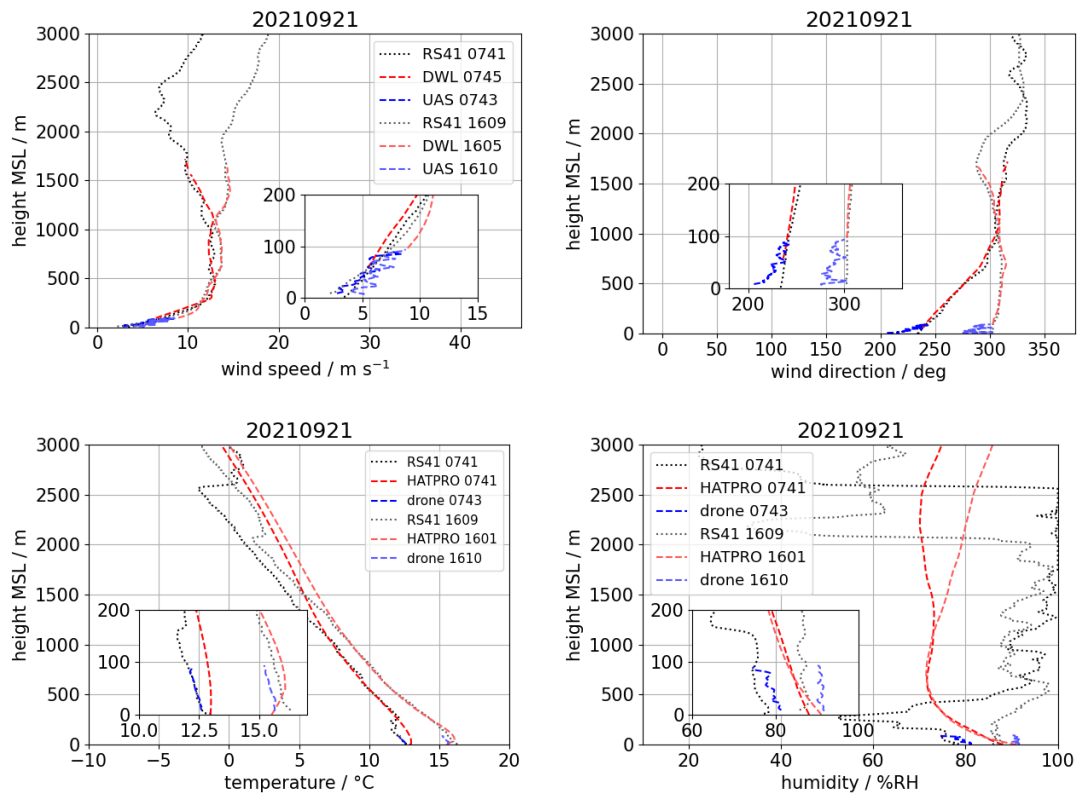


**Figure 2.** Comparison of wind speed (a), wind direction (b), temperature (c) and humidity (d) measurements of two radiosonde launches (grey) and two UAS flights (blue) on 21 September 2021 with remote sensing data from DWL and MWR (red).

#### 4.2. Validation of remote sensing measurements

To validate the remote sensing data prior to the installation of measurement masts at the WiValdi site, a two-week long campaign was carried out in September 2021. 14 radiosondes were launched in this period and in parallel to each radiosonde launch, a meteorological multicopter UAS (see [9]) was launched to obtain soundings in the lowest 100 meters. The radiosonde data up to 10 km are particularly useful to assess the performance of the MWR retrievals. As an example, Fig. 2 shows the comparison of radiosonde (RS41), UAS and remote sensing measurements for two flights on 21 September 2021. The DWL measurement height strongly depends on the aerosol content and cloud level in the atmosphere so that at this day, a maximum height of 1700 m could be reached. The MWR continuously provides data up to 10 km, but small-scale fluctuations and strong gradients such as temperature inversions at the boundary-layer top cannot be captured very well. Nevertheless, the lapse rate in the lower boundary layer is represented satisfactorily. The humidity retrieval is subject to large uncertainties. This is reflected in large deviations that were measured in comparison to the radiosonde (see Fig 2d). Humidity data is not used for further analyses in this study and needs to be improved with future retrievals.

### 4.3. Wind and turbulence statistics

4.3.1. *Overall statistics* We compare the wind rose at 100 m height above ground of the lidar observations to the long-term wind statistics of the NEWA mesoscale simulation output at 100 m (2011-2018, [10]). Figure 3 shows that both sources feature an accumulation of westerly winds, but also a significant portion of easterly winds. In the observational period, weak winds from northwest were observed more frequently than southwest wind directions, which is different compared to the long-term simulation. This difference can be attributed to the synoptic situation in 2021, which was impressed by many low pressure systems passing over Central Europe in the months from March to August. The strong winds from the East in the DWL data can mainly be attributed to winter storms that occurred in February 2021.

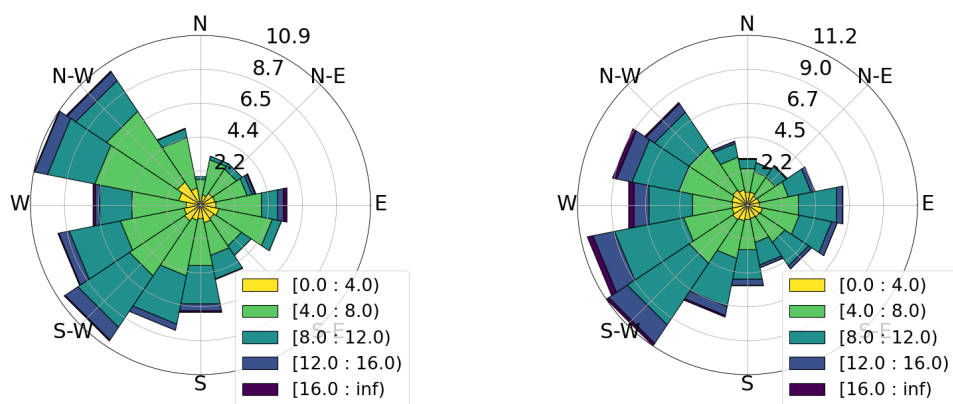


**Figure 3.** Wind roses from lidar measurements (left) and NEWA mesoscale simulations (right) at 100 m agl.

Turbulence kinetic energy (TKE) is calculated from lidar measurements and is available as model output from NEWA. For the WiValdi site, the historic NEWA data and the recent lidar measurements do not show any significant differences. The distribution of TKE is almost the same over all wind directions, with no outstanding wind sector for increased turbulence (Fig. 4).

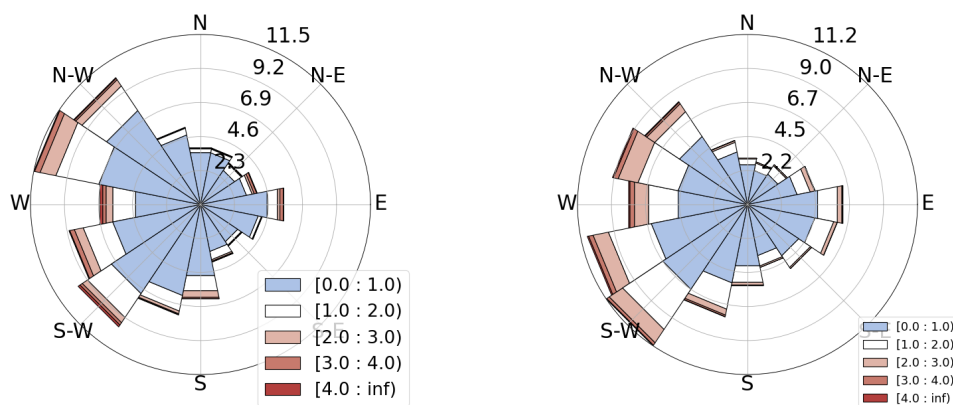


**Figure 4.** TKE roses from lidar measurements (left) and NEWA mesoscale simulations (right) at 100 m agl.

The statistics of the lapse rate at hub height reveal that similar to the findings of Emeis et al. (2016) [4] and Platis et al. (2021) [3] for the German Bight, the stable cases are found much more regularly in conditions with southerly and easterly winds and offshore winds from the North Sea mostly feature neutral or even unstable stratification. Both sources, model and MWR measurements agree with this general feature of the site (see Fig. 5).

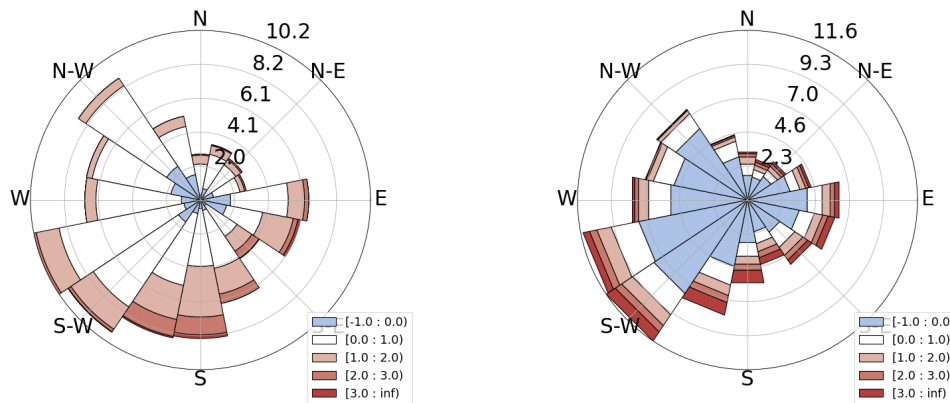


**Figure 5.** Stability roses from MWR measurements (left) and NEWA mesoscale simulations (right) at 100 m agl.

The monthly mean winds and their standard deviation show a weak annual cycle in both, the model results and the measurements, with slightly lower mean winds in summer (Fig. 6).

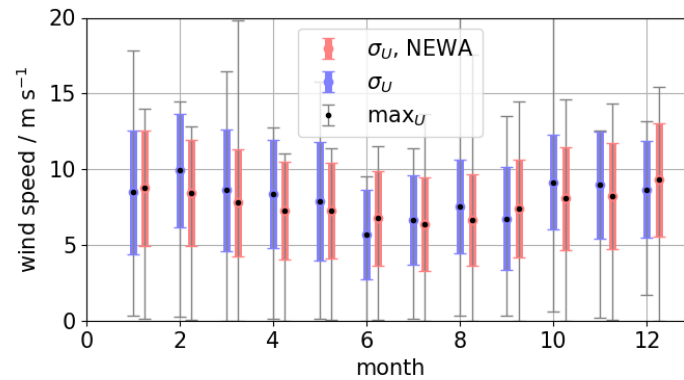


**Figure 6.** Monthly mean, standard deviation and maximum wind speeds in comparison of lidar and NEWA data.



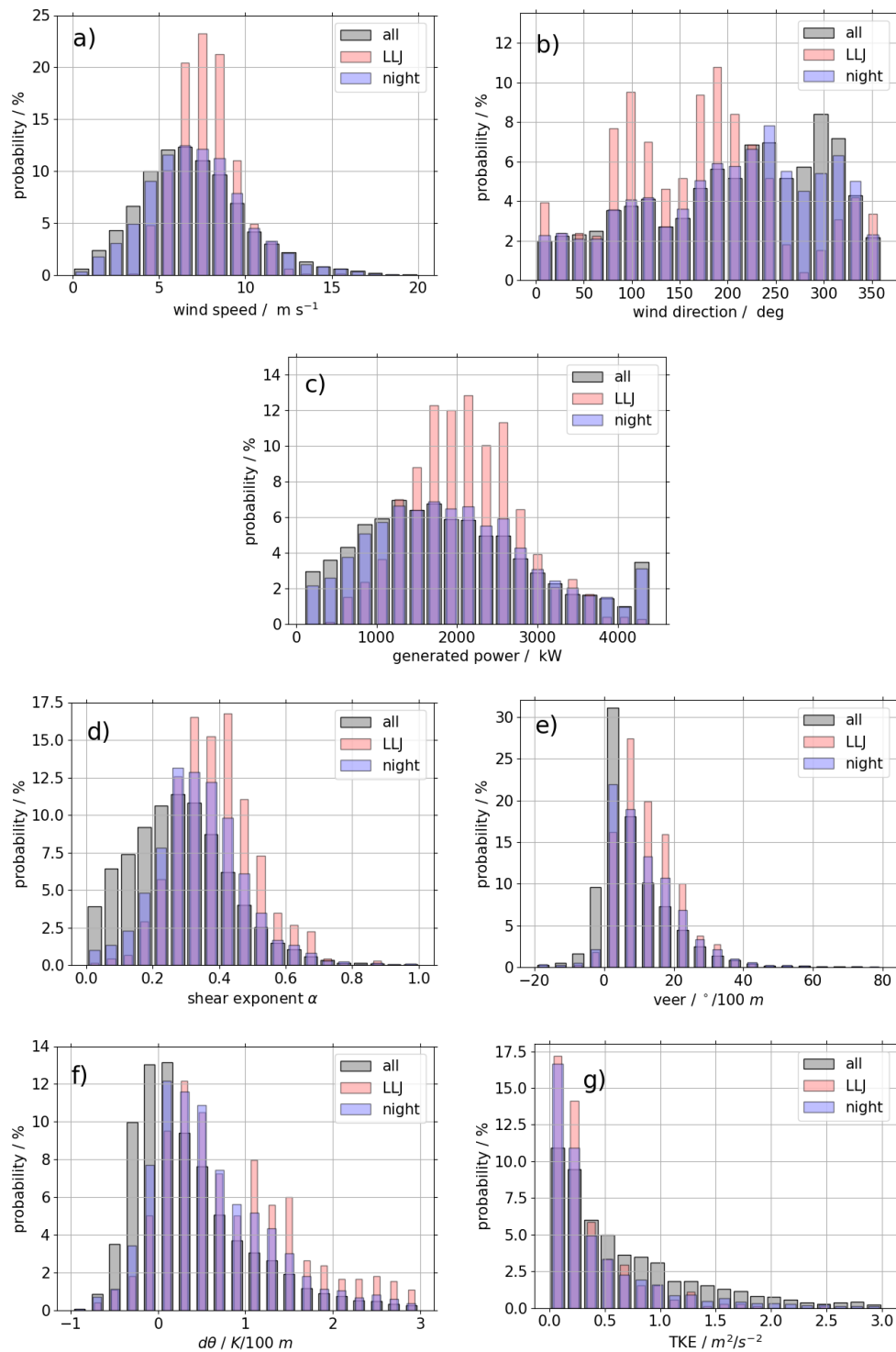


**Figure 7.** Histograms of wind speed (a), wind direction (b), wind shear (c) and veer (d), lapse rate (e) and TKE (f) for the whole measurement period (grey), only nighttime cases (blue) and LLJ events (red).

*4.3.2. Discrimination of nighttime and daytime regimes* The atmospheric stratification is crucial for the shape of the wind profile and turbulence. For this reason we discriminate nighttime (sunset to sunrise) and daytime regimes, in order to evaluate the specific load cases in different conditions. A special case are LLJ situations, which can occur frequently at the WiValdi site. We filtered LLJ data according to the detection algorithm described in Sect. 3.1.3. The histograms in Fig. 7 show that wind speed at 100 m is almost equally distributed in nighttime regimes compared to the overall dataset with only a small shift to higher wind speeds. As expected, nighttime stratification is shifted towards more stable cases, which goes along with higher shear and veer, but lower turbulence. The average wind shear exponent in the overall dataset is  $\alpha = 0.25$ , with a distribution that is quite similar to what Kelley et al. (2014) described for the Høvsøre site (see Fig. 8 and [11]). With only the nighttime data, the shear exponent is significantly higher ( $\alpha = 0.31$ ). Correspondingly, average wind veer increases from  $\Delta\Psi = 7.5^\circ$  to  $\Delta\Psi = 10.4^\circ$ . Translated into generated power according to Sect. 3.1.4, the distribution in Fig. 7c shows that most of the power can be expected to be generated in partial load conditions. Approximately 3% of the time, the WT operates at the rated power. As for wind speeds, the differences between daytime and nighttime are small.

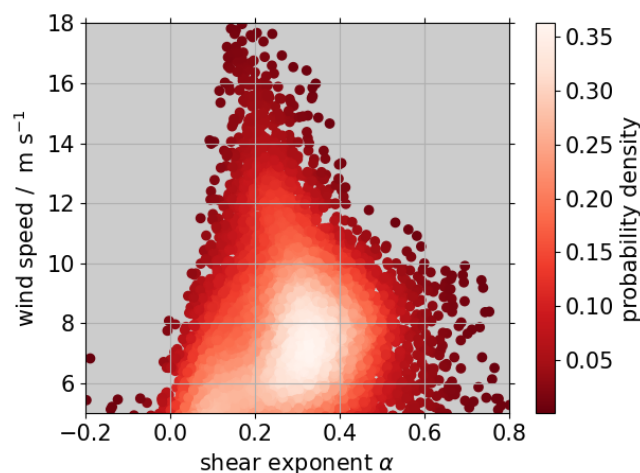


**Figure 8.** Scatter plot of wind speed versus wind shear for DWL measurements from December 2020 through November 2021. Color coded is the probability of occurrence.

*4.3.3. Nighttime low-level jet analyses* The analysis of LLJ statistics shows that occurrences of LLJ events can be detected on 49 % of the days. It is striking that LLJs occur with a significantly higher probability in the wind sectors from  $70^\circ$  to  $200^\circ$  which feature a long fetch over land (see Fig. 7). Especially the two sectors that are indicated in yellow in Fig. 1 show a large number of LLJ events. On the contrary, almost no LLJ events are detected in the wind sector  $270^\circ$ - $320^\circ$  which features landward winds from offshore and is indicated in green in Fig. 1.

The average height of the jet maximum is at approx. 400 m but varies on a wide range between 100 m and 600 m. Very low LLJs cannot be detected well due to the lowest measurement height of 57 m with the DWL and should be considered in future studies when meteorological masts will be available on site. Average shear and veer increase to  $\alpha = 0.37$  and  $\Delta\Psi = 12.2^\circ$  in LLJ conditions, but values of  $\alpha \geq 0.5$  and  $\Delta\Psi \geq 20^\circ$  are not uncommon. Figure 9 gives scatter plots of LLJ height, veer, shear and maximum wind speed in the LLJ in dependency of the potential temperature gradient  $\Delta\theta$ . LLJ height decreases with increasing stability, whereas shear and veer

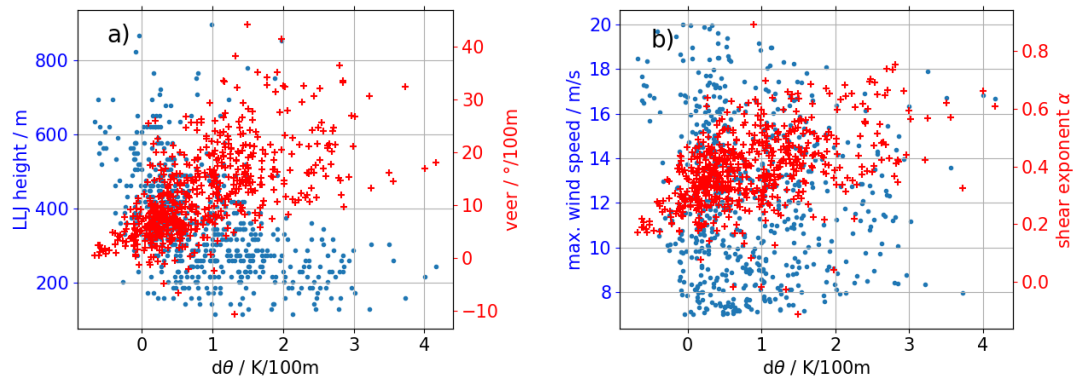


**Figure 9.** Scatter plots of LLJ height (blue) and veer (red) over lapse rate (a) as well as LLJ maximum wind speed (blue) and wind shear (red) over the lapse rate (b).

increase. There is no obvious correlation between maximum wind speed and stability.

## 5. Conclusions

We showed that the combination of a DWL with a MWR can be used to capture meteorological conditions in the ABL over a long period and derive significant statistical information for enhanced site assessment. A focus of the analyses was put on wind and stability conditions at hub height of the future research WTs at the site. We showed that the wind conditions at the WiValdi Research Wind Farm show some features which were previously observed in the German Bight. Landward wind from the North Sea is mostly neutrally stratified when it reaches the site, whereas seaward winds from southwest to southeast is more often found with stable stratification, especially at night, as it is common over land in the North German Plain. In nights with a stably stratified ABL, LLJs occur frequently, i.e. in 49% of the days, and cause increased wind shear and veer in the rotor area. A deeper analysis of synoptic and mesoscale atmospheric conditions is necessary in future to understand the interaction of inertial oscillation and land-sea effects that form the LLJs at the WiValdi site. The advantage of long-range DWL and MWR measurements over conventional instrumentation like meteorological masts is that their measurements reach up to larger heights, so that a better understanding of the atmospheric situation throughout the ABL and at least for temperature, the whole troposphere can be obtained. It needs to be shown in future however, if those 10-20% of missing data due to adverse weather conditions for DWL measurements are of concern for the estimation of wind resources. Furthermore, uncertainties of the MWR measurements in temperature close to the surface and especially humidity measurements need to be further analysed and improved in future. For this purpose, the additional in-situ and remote sensing instrumentation which is planned for WiValdi can be used. Sensors below 60 m at the masts will then also allow to study LLJs with wind speed maxima at low altitudes.

Already now, the dataset which was collected at the WiValdi Research Wind Farm prior to installation of wind turbines and meteorological masts is an asset to future research at the site. The combination of wind, temperature and humidity profiles provides a full thermodynamic state of the ABL. Such data can potentially also be assimilated into NWP models and improve mesoscale forecasting capabilities in future. Continued measurements after WT installation will be an important part of the monitoring of atmospheric conditions in the wind farm during its operation and a variety of research is conceivable that uses this data for power performance analyses or in short-term forecasts.

## Acknowledgments

This work was performed within projects DFWind, funded by the Federal Ministry of Economy and Energy on the basis of a resolution of the German Bundestag under the contract number 0325936A.

## References

- [1] The International Electrotechnical Commission 2021 Assessment of wind resource, energy yield and site suitability input conditions for wind power plants Tech. Rep. IEC 61400-15
- [2] Klassen J, Tessmer J, Barzgaran B, Dittmer A, Gerz T, Hach O, Herr M, Imiela M and Willberg C 2022 *Journal of Physics: Conference Series* accepted for publication
- [3] Platis A, Hundhausen M, Lampert A, Emeis S and Bange J 2021 *Boundary-Layer Meteorol* **182** 441–469
- [4] Emeis S, Siedersleben S, Lampert A, Platis A, Bange J, Djath B, Schulz-Stellenfleth J and Neumann T 2016 *Journal of Physics: Conference Series* **753** 092014
- [5] Kalverla P C, Duncan Jr J B, Steeneveld G J and Holtslag A A M 2019 *Wind Energy Science* **4** 193–209
- [6] Wildmann N, Päsche E, Roiger A and Mallaun C 2020 *Atmospheric Measurement Techniques* **13** 4141–4158
- [7] Crewell S and Lohnert U 2007 *IEEE Transactions on Geoscience and Remote Sensing* **45** 2195–2201
- [8] RPG 2015 Instrument operation and software guide Tech. rep. Radiometer Physics
- [9] Wetz T, Wildmann N and Beyrich F 2021 *Atmospheric Measurement Techniques* **14** 3795–3814
- [10] Witha et al B 2019 WRF model sensitivity studies and specifications for the NEWA mesoscale wind atlas production runs
- [11] Kelly M, Larsen G, Dimitrov N K and Natarajan A 2014 *Journal of Physics: Conference Series* **524** 012076